

Revista Mexicana de Ingeniería Biomédica

Volumen
Volume 24

Número
Number 1

Marzo
March 2003

Artículo:

Dielectrophoretic field-fractionation of rouleaux formed of human rythrocytes: A feasibility study

Derechos reservados, Copyright © 2003:
Sociedad Mexicana de Ingeniería Biomédica, AC

Otras secciones de
este sitio:

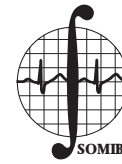
- 👉 [Índice de este número](#)
- 👉 [Más revistas](#)
- 👉 [Búsqueda](#)

*Others sections in
this web site:*

- 👉 [Contents of this number](#)
- 👉 [More journals](#)
- 👉 [Search](#)



Medigraphic.com



Dielectrophoretic field-fractionation of Rouleaux formed of human erythrocytes: A feasibility study

Araceli Ramírez,* Alfred Zehe,** Oleg Starostenko***

* Instituto de Ciencias.

** Facultad de Ciencias Físico Matemáticas.

*** Universidad de las Américas, UDLA, Centro de Investigación CENTIA.

Benemérita Universidad Autónoma de Puebla.

Correspondencia:

Araceli Ramírez, Alfred Zehe
17 Oriente No. 1603, Puebla, Pue.,
México. Tel. 229-55-00 ext. 7851;
Fax. 244-34-66.

E-mail: eduardors@prodigy.net.mx

ABSTRACT

Red blood cell (RBC) aggregation, and specifically linear Rouleaux formation of human erythrocytes affects the rheology of microcirculation and has been widely studied in order to quantify flow abnormality in pathological conditions. Rouleaux form through side-by-side adhesion of a considerable number of erythrocytes and may reach a roll length of 50 μm and more. This compares to the 2.2 μm in thickness of common RBC's. Increased aggregation of RBC's may be an important factor in the development of vascular diseases and microcirculation impairment. Dielectric properties of cell suspensions or of undiluted whole blood are strongly related i.e. to the geometrical structure of particles. Electrophoretic measurements of Rouleaux in various suspending media have the potential of size-characterization and spatial separation of cell subpopulations. In the present paper we show, that the electrophoretic force on RBC aggregations of different size, exposed to an electric field of variable frequency, provides a means for a spatial separation and sorting of Rouleaux with different "stack number" of aggregated erythrocytes. In particular is the field-flow-fractionation technique a suitable tool, where the differential positioning of particles within a suspension flow velocity profile is established by the action of corresponding dielectrophoretic forces.

Key Words:

Human erythrocytes, Rouleaux, Dielectrophoresis, Force effects, Sorting and separation.

RESUMEN

La agregación de glóbulos rojos (RBC), y específicamente la formación de Rouleaux lineares de eritrocitos afecta la reología de la microcirculación y ha sido ampliamente estudiada para cuantificar anomalías de flujo en condiciones patológicas. Los Rouleaux se forman por adhesión, por contacto de un número considerable de eritrocitos y pueden alcanzar una longitud de rollo de 50 μm o más. Esto se compara al grosor común de 2.2 μm de los RBC's comunes. La agregación aumentada de RBC's puede ser un factor importante en el desarrollo de enfermedades vasculares y alteraciones de la microcirculación. Las propiedades dieléctricas de suspensiones celulares o de sangre sin diluir están estrechamente relacionadas con la estructura geométrica de las partículas. Mediciones electroforéticas de Rouleaux en varios medios de suspensión tienen el potencial de caracterizar el tamaño y la separación

espacial de sub-poblaciones celulares. En el presente trabajo mostramos que la fuerza electroforética en agregaciones RBC de diferente tamaño, expuestas a un campo eléctrico de frecuencia variable, provee un medio para la separación espacial y la clasificación de Rouleaux con diferente "número de stack" de eritrocitos agregados. En particular, la técnica de fraccionamiento del flujo de campo es una herramienta adecuada, donde el posicionamiento diferencial de las partículas en suspensión dentro del perfil de velocidad de flujo es establecido por la acción de las fuerzas dielectroforéticas correspondientes.

Palabras clave:

Eritrocitos humanos, Rouleaux, dielectroforesis, efectos de fuerza, separación y clasificación.

INTRODUCTION

Erythrocyte aggregation and the formation of linear Rouleaux has been widely investigated, and its importance in the rheology of blood circulation is well established¹⁻⁴. The acting aggregation forces have been studied⁵⁻⁷, and measurable effects of zero gravity under space condition on the human erythrocyte Rouleaux formation were detected⁸. Observation show, that human and horse RBC's form stable Rouleaux, whereas bovine RBC's do not aggregate in plasma⁹. A controlled formation of erythrocytes doublets by electrofusion has been reported recently¹⁰. The size of such "coin stacks" is of clinical relevance^{11,12}, stimulating interest in their analysis and manipulation. Methods based on dielectric properties of dispersed systems are widely used to investigate the kinetics of RBC aggregation and break-up^{13,14}.

The spatial separation of polarizable particles and biological cells by dielectrophoresis has been demonstrated by a number of research groups. This includes a range of microorganisms¹⁵⁻¹⁷, mammalian cells¹⁸⁻²⁰, and microscopic polystyrene and latex spheres^{21,22}. Combined electrophoretic and dielectrophoretic forces are applied to trap and manipulate single particles of DNA on special microelectrodes²³⁻²⁵. The advancement and use of microelectronics technologies in bioelectronic analysis devices is leading to efficient and effective methods for the direct manipulation, separation and sorting of submicron particles on high integrated semiconductor chips²⁶⁻²⁹.

The dielectric properties of a particle, suspended in a conductive medium, and exposed to an electric field of special characteristics determine the direction of movement and the acting absolute force on it. The knowledge of the internal elec-

tric field strength is a basic aspect of the study of many biological effects. The shape of the sample has a strong impact on it. Spherical and ellipsoidal cells models are frequently used due to the fact that linearly polarized electric plane waves generate a uniform local field distribution accessible by closed analytical solutions of the Laplace equation³⁰⁻³².

However same biological cells, including erythrocytes, deviate from the ellipsoidal form, and in order to account for these special shaped cells, more satisfactory cell models with shapes close to disks or cylinders³³⁻³⁵ have been considered.

Rouleaux of erythrocytes, often quoted as linear "coin stacks" translate into a cylindrical cell model. Characterized by an integer number of single cell heights, the aggregation of three or more cells changes the cell geometry in an ellipsoidal model from oblate to prolate. The local field and the induced dipole moment is thus affected considerably.

In this paper we show, that the multiplicity of erythrocyte cell aggregates can be followed up by dielectrophoresis, and a size-selective separation can be achieved, given correct medium permittivity and conductivity, as well as frequency and amplitude of the applied electric field. While the approximation of larger erythrocyte Rouleaux as general spherical ellipsoids might be sufficient, an approximation procedure for dielectric bodies of short cylindrical shape is described by us and applied on stacks of erythrocytes with variable height-to-radius relation.

DIELECTROPHORETIC FORCE

The movement of an object caused by a spatially non-uniform electric field, is often called dielectrophoresis (DEP). It is different from the well-known

phenomenon of electrophoresis, because DEP only arises, when the object has a different tendency to become electrically polarized relative to its surrounding medium. Positive DEP means, the object will be pulled towards higher electrical field regions, if its polarizability is higher than that of the suspending medium. Conversely it will be repelled towards weak field regions, if its polarizability is lower. Objects can thus be trapped by positive DEP, or concentrated in a focal point by negative DEP, or even levitate in a moving medium. Different subpopulations of particles can be moved apart from each other and spatially separated in three dimensions, given the application of appropriate field and suspending medium conditions^{27,35}.

Dielectrophoretic forces are caused by the interaction of non uniform electric fields with dielectric objects, which are suspended and free to move in a conductive medium. In inhomogeneous A.C. fields, the time averaged force $\langle \vec{F} \rangle$, which is acting on a homogeneous dielectric particle, can be expressed by

$$\langle \vec{F} \rangle = \frac{1}{2} \operatorname{Re} \{ \vec{m} \cdot \nabla \vec{E}^* \} \quad (1)$$

where \vec{m} is the induced dipole moment, $\nabla \vec{E}$ is the gradient of the complex conjugate of the external field, and Re denotes the real part of the scalar product. The induced dipole moment \vec{m} is proportional to the particle volume V , the acting external electric field $E = E_0 \cdot e^{j\omega t}$ of circular frequency ω , and the permittivity $\epsilon_0 \epsilon_m$ of the medium surrounding the dielectric object.

The time-averaged force acting on a homogeneous ellipsoidal particle is given by

$$\langle \vec{F}_{DEP} \rangle = \epsilon_0 \epsilon_m \cdot V \cdot \operatorname{Re} \{ K(\omega) \} \nabla |E_{rms}|^2 \quad (2)$$

with

$$K(\omega)_x = \frac{\epsilon_p^* - \epsilon_m^*}{\epsilon_m^* + (\epsilon_p^* - \epsilon_m^*) \cdot n_x} \quad (3)$$

the component in x-direction of the Classius-Mossotti factor. ϵ_p^* is the complex permittivity of the particle, and n_x is the Lorentz depolarization factor in this direction, parallel to the external field. The Classius-Mossotti factor is a measure of the effec-

tive polarizability of the particle, and depends for n_x strongly on the geometrical shape of the ellipsoidal object. With ϵ the permittivity and s the electrical conductivity of any dielectric medium, the complex permittivity ϵ^* is defined as

$$\epsilon^* = \epsilon_0 \epsilon - j(s/\omega) \quad (4)$$

being j the imaginary unit $(-1)^{1/2}$.

Consequently, the Classius-Mossotti factor depends on the frequency of the applied field, besides the dielectric properties of particle and medium. When only frequency dependencies are the aim of the study, it is sufficient to consider $K(\omega)$ as the only frequency-dependant part of the induced dipole moment. Variations of this factor give rise to the dielectrophoretic force described in (2), which is unique to a special particle type. This concerns not only intrinsic dielectric properties, but also the geometrical shape via the depolarization factors and the size via the volume contained in the induced dipole moment.

Shape and size variation of the particles affect $K(\omega)$ and modify V , which leads to readily achievable dielectrophoretic separations protocols. The design and geometry of the microelectrodes used to generate and control the non-uniform electric fields is of course an important factor to be considered.

From expression (3) follow two special cases of practical importance: at the one hand sphere-shaped particles with $n_x = n_y = n_z = 1/3$, yielding

$$\langle F_{DEP} \rangle_{sphere} = 2\pi r^3 \epsilon_0 \epsilon_m^* \operatorname{Re} \left\{ \frac{\epsilon_p^* - \epsilon_m^*}{\epsilon_p^* + 2\epsilon_m^*} \right\} \nabla |E|^2 \quad (5)$$

and at the other hand long cylinder-shaped particles with $n_x = 0$, ($n_y = n_z = 0.5$)

$$\langle F_{DEP} \rangle_{rod} = \frac{\pi r^2 \ell}{3} \epsilon_0 \epsilon_m^* \operatorname{Re} \left\{ \frac{\epsilon_p^* - \epsilon_m^*}{\epsilon_m^*} \right\} \nabla |E|^2 \quad (6)$$

where ℓ is the length, and r is the radius of the cylinder. It is clear, that the applicability of expressions (5, 6) has to be verified with respect to the particle shape in any practical approach. For instance is the herpes simplex virus, HSV-1, a spherical enveloped particle, whereas the tobacco mosaic virus,

TMV, is a 280 nm-long protein tube of 18 nm diameter (long cylinder).

HUMAN ERYTHROCYTE ROULEAUX

The calculation of force effects on biological cells starts commonly with a solution of the Laplace equation under quite restrictive conditions. In order to arrive at closed expressions, and ellipsoidal cell model with a confocal shell as commonly assumed, as only such a geometry exhibits a constant local field. Normal human erythrocytes are non-nucleated biconcave disk-shaped cells of about $7.5 \mu\text{m}$ in diameter with edges that are thicker than the center part (Figure 1). Indeed, they resemble an oblate ellipsoid only in a crude approach. The determination of the induced dipole moment for such a structure in field direction will be possible only to a certain approximation, e.g., of a very short circular cylinder (flat disk) of radius R and half length L with $L/R < 1$.

The aggregation of disk-shaped objects to columns has a clear effect on the local field and the induced dipole moment. While the depolarization factor in direction of the Rouleaux (cylinder) axis parallel to the external electric field takes a value close to 0 for $L/R \gg 1$, leading to expression (6), for a disk-shaped body, this value is closer to 1.

In linearly polarized A.C. fields, particles are oriented along their axis of highest polarization. A long cylinder will line up with its symmetry axis along the field, while a circular disk lines up along its radius. The orientation of a cube-like object (cylinder with $L/R = 1$) results uncertain, though (Figure 2).

It is important to remember, that the side-by-side aggregation of individual erythrocytes generates columns of length $l = s \cdot d$ with d the thickness of a single cell ($d = 2.2 \mu\text{m}$) and stack number $s = 1, 2, 3, \dots$. While single or double erythrocytes orient themselves along the radius on the mayor axis, aggregations of more than three erythrocytes results in cylinder-shaped structures with $L > R$. Depending on the number s , the axis ratio of the Rouleaux, L/R , the depolarization factor and the induced dipole moment change correspondingly, and so does the dielectrophoretic force acting on any of the Rouleaux. For the sake of simplicity, only electric effects are considered here, although hydrodynamic friction or motions induced by temperature fields are not without importance, particularly at elevated medium conductivities.

In order to arrive at quantifying expressions of the DEP force (expression (1), we have to determine the size dependent polarization of cylinder-shaped Rouleaux. This is in the context of the present paper a tedious endeavor, and we will restrict ourselves to a sketchy description of the result in the following chapter.

DIPOLE MOMENT OF A CYLINDER-SHAPED (NON-ELLIPSOIDAL) DIELECTRIC BODY

The common approach for the determination of the induced polarization in order to arrive at expressions related to force actions or a special dielectric object is the assumption of an ellipsoid with half-axis a, b, c as substituting body shape. In this so-called Laplace model, a homogeneous ellipsoid

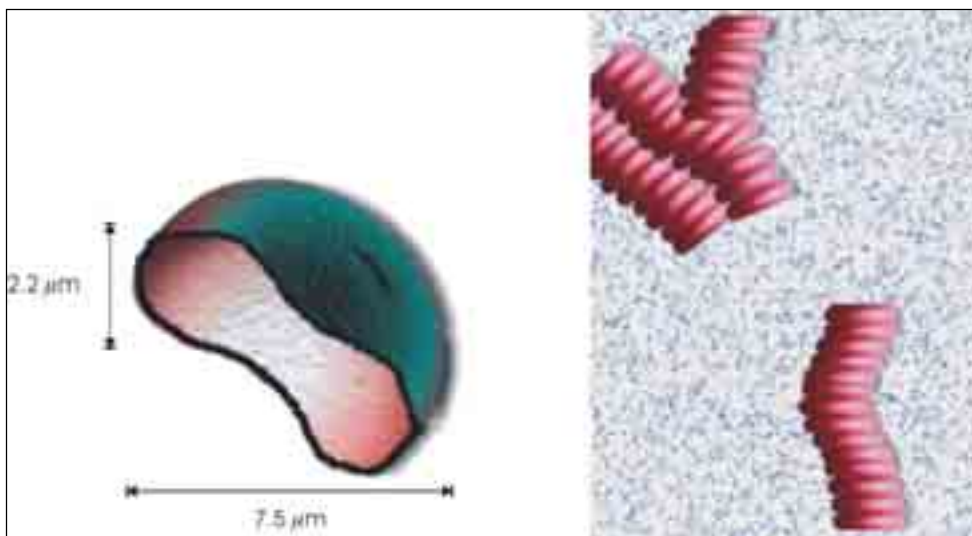


Figure 1. (a) Transverse section of an erythrocyte with radius R and thickness d . (b) Rouleaux of erythrocyte formed through side-by-side adhesion of single RBC's.

always exhibits a constant local (internal) field. Integration over this field leads to the induced polarization and thus to expressions related to force actions on the special object. But already in such important cases as for a cube or a short cylinder is it difficult to calculate the depolarization factors. But even then is the best shape of it to be used, and the next approximation step, not a straightforward choice. This chapter deals with an approximation procedure for the calculation of the internal (local) field $\vec{E}_i(\vec{r})$ in a material body of general shape, as e.g. a cylinder shaped rouleaux having a dielectric constant ϵ_p^* , which is brought into a given field $\vec{E}_0(\vec{r})$, acting inside a suspending medium of dielectric permittivity ϵ_m^* .

The problem can be formulated as follows: The local field $\vec{E}_i(\vec{r})$ causes a polarization $\vec{P} = \epsilon_0(\epsilon_p^* - \epsilon_m^*)\vec{E}_i$ of the rouleaux. On an surface element $d\vec{F}$ of the dielectric body, this polarization generates a polarization charge $dq = \epsilon_{pol} \cdot d\vec{F} = \vec{P} \cdot d\vec{F}$ which by virtue of the Coulomb law, together with the unperturbed field $\vec{E}_0(\vec{r})$, produces the local field such that

$$\vec{E}_i(\vec{r}_1) = \vec{E}_0(\vec{r}_1) - \iint \frac{\vec{r}_{12}}{4\pi\epsilon_0 r_{12}^3} [\vec{P}(\vec{r}_2) \cdot \Delta \vec{F}_2] \quad (7)$$

The integration is carried out over the surface of the dielectric body; $d\vec{F}$ points outward, and \vec{r}_{12} combines the origin \vec{r}_1 with the integration element at \vec{r}_2 . The relation between $\vec{E}_0(\vec{r})$ and $\vec{E}_i(\vec{r})$ is supposed by us to be linear, thus

$$\vec{P}(\vec{r}) = \epsilon_0(\epsilon_p^* - \epsilon_m^*)\vec{E}_i(\vec{r}) = \epsilon_0(\epsilon_p^* - \epsilon_m^*)\alpha(\vec{r})\vec{E}_0(\vec{r}) \quad (8)$$

In general, $\alpha(\vec{r})$ is a tensor, as the directions of \vec{E}_i and \vec{E}_0 are not necessarily parallel.

Exact solutions with a constant α are known for

the sphere, the infinitesimal thin wire (needle), and the infinitesimal extended disk (sheet). When our approach is applied here, already the first approximation step gives the exact solution, as it should, when $\alpha(\vec{r}) = \alpha_1 = \text{constant}$.

The polarization of a prolate spheroid (Figure 3a) results with expression (8) and the axis relation $q^2 = b^2 / (a^2 - b^2)$ in

$$\alpha = \left\{ \epsilon_m + (\epsilon_p^* - \epsilon_m^*)q^2 \left(1 + \frac{\sqrt{q^2 + 1}}{2} \cdot \ln \frac{\sqrt{q^2 + 1} - 1}{\sqrt{q^2 + 1} + 1} \right) \right\}^{-1} \quad (9)$$

For an oblate ellipsoid one gets instead

$$\alpha = \left\{ \epsilon_m + (\epsilon_p^* - \epsilon_m^*)(q^2 + 1) \left(q \arctan \frac{1}{q} - 1 \right) \right\}^{-1} \quad (10)$$

and consequently with $q \rightarrow \infty$ (or $a = b$) we have for the sphere-shaped dielectric

$$\alpha_1 = 3 / (\epsilon_p^* + 2\epsilon_m^*)$$

yielding the known expression for the polarization vector

$$\vec{P} = 3\epsilon_0 \frac{\epsilon_p^* - \epsilon_m^*}{\epsilon_p^* + 2\epsilon_m^*} \cdot \vec{E}_0 \quad (11)$$

It is easy to recognize, that $K(w) = 3(\epsilon_p^* - \epsilon_m^*) / (\epsilon_p^* + 2\epsilon_m^*)$, the Classius-Mossotti factor, is in accord with expressions (2, 5).

The full application of the approximation procedure for a cube or short cylinder requires several

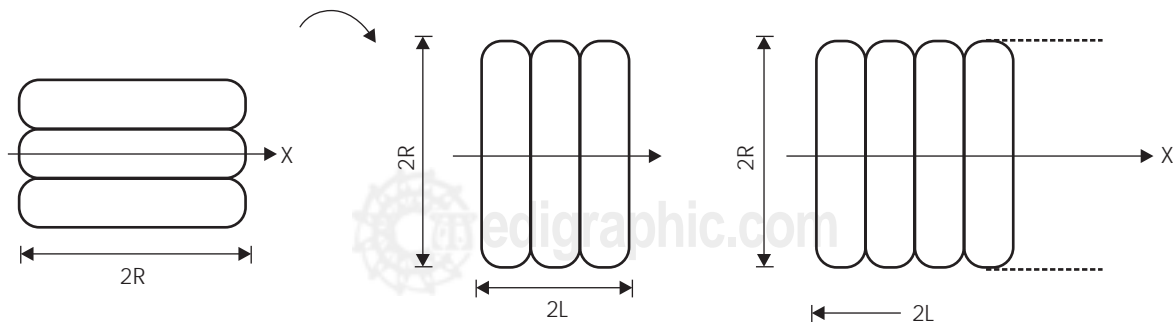


Figure 2. Schematic presentation of erythrocyte Rouleaux of length $2L = S \times d$. Direction of maximum polarization is x. For $s = 1, 2, 3$ the radius R of the cell aggregation aligns with the external field. d is the thickness of a single erythrocyte, R its radius.

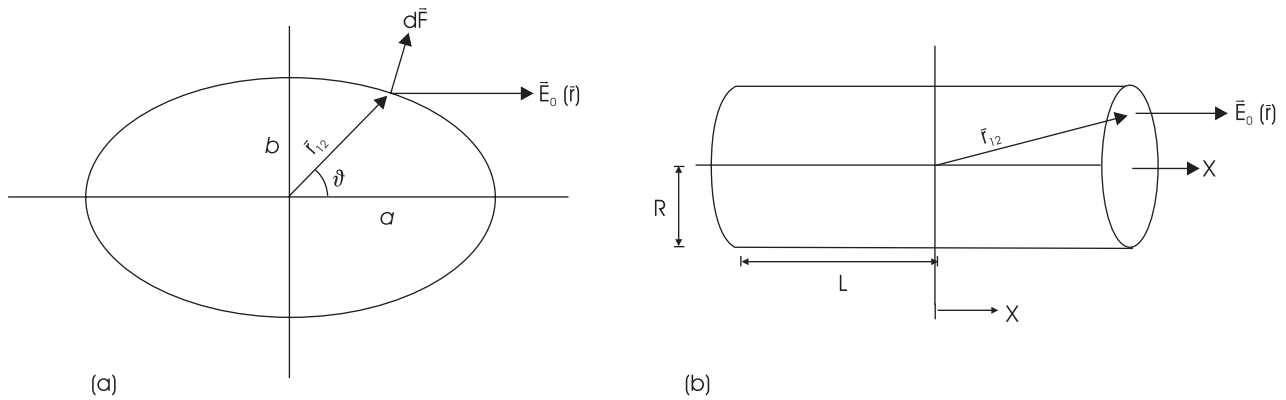


Figure 3. (a) Prolate ellipsoid; and (b) dielectric cylinder of diameter $2R$ and length $2L$.

steps and leads to a somewhat unhandy but more exact result. It will not be carried out here, and only the final result of the dipole moment of a cylinder of radius R and half-length L (see Figure 3b) is given in expression (12).

$$\bar{m} = V \cdot \bar{P} = \pi R^2 \epsilon_0 (\epsilon_p^* - \epsilon_m^*) \left\{ \epsilon_m^* + (\epsilon_p^* - \epsilon_m^*) \left[1 - (1 + R^2 / L^2)^{-1/2} \right] \right\}^{-1} E_0^* * \left\{ 2L + \frac{L - 2L(1 + R^2 / L^2)^{-1/2} - L(1 + 8L^2 / R^2)^{-1} + (R^2 + 2L^2) \cdot (R^2 + 4L^2)^{-1/2} - R}{(\epsilon_p^* - \epsilon_m^*)^{-1} + 1 - 7/16(1 + 11R^2 / 56L^2)} \right\} \quad (12)$$

In the case of human erythrocyte Rouleaux the only parameter which varies is L . We will use the symbol S as the stacking number of erythrocytes, forming Rouleaux of half-length $L = S \times (\frac{1}{2}d)$, where $d = 1.1 \text{ mm}$, half the thickness of a single erythrocyte.

Corresponding to the tendency, the dielectric bodies align its axis of maximum polarization with the external field, cell aggregates up to a stacking number $S = 3$ will have the direction of the single cell radius parallel to the external field, while for $S \geq 4$, the cylinder axis aligns with the field (see Figure 2).

DIELECTROPHORETIC FORCE AND DISCUSSION

The frequency response of the DEP force on linear arrangements of erythrocyte "coin stacks" is governed by expressions (2), (14) and the corresponding Clausius-Mossotti factor, which is related to a by

$$K(\omega) = a \cdot (\epsilon_p^* - \epsilon_m^*) \quad (13)$$

In the limiting cases of a long cylinder (needle) and a sphere, with $a = 1/\epsilon_m^*$ and $a = 3/(\epsilon_p^* - \epsilon_m^*)$, respectively, the relations (5, 6) are of course reproduced. In the following calculus the Rouleaux are

approximated to solid homogeneous cylinders of length $2L = s \times d$ (Figure 2) with a relative permittivity $\epsilon_p = 50$ and conductivity $s_p = 0.5 \text{ S/m}^{30}$.

Using these parameters, a plot of the frequency variation of the polarization factor, estimated from expression (13) was calculated as a function of frequency and Rouleaux-length parameter s at different aqueous medium conductivities s_m between 0.001 and 0.1 S/n . The results for the dielectrophoretic force, which is proportional to $S \times \text{Re}[K(\omega)]$, are shown in the following figures.

The medium conductivity s_m is an essential process parameter, as it can be seen in Figures 4 and 5, where $s_m = 0.1 \text{ S/m}$ and 0.001 S/m , respectively.

The force on rouleaux, characterized by the stack-parameter S of erythrocytes, is expectedly quite different for different Rouleaux length. It depends also in the conductivity of the suspending medium, being larger in lower conductive liquids. Comparing e.g. the Rouleaux with $S = 10$ in the two media shows a DEP force almost twice as high in the $s_m = 0.1 \text{ S/m}$. As shown in Figures 4(b) and 5(b) with more detail, the difference in the critical frequencies (defined as frequencies, where the DEP force passes through zero, $S \times \text{Re}[K(\omega)] = 0$) of rouleaux, formed of say 7 or 8 erythrocytes is about 4 MHz, a technical value easy to control under experimental conditions. A certain "crowding" of curves is seen with $s = 1, 2$ and $s = 3, 4$ in Figure 4(b), or with $s = 2, 3$ in Figure 5(b), which is a consequence of the reorientation of very short Rouleaux. The tendency to align the major particle axis with the external field has been demonstrated in Figure 2. By comparing Figures 4(b) and 5(b) the "crowding" between determined Rouleaux lengths can be relieved by choosing suspending media of different conductivity.

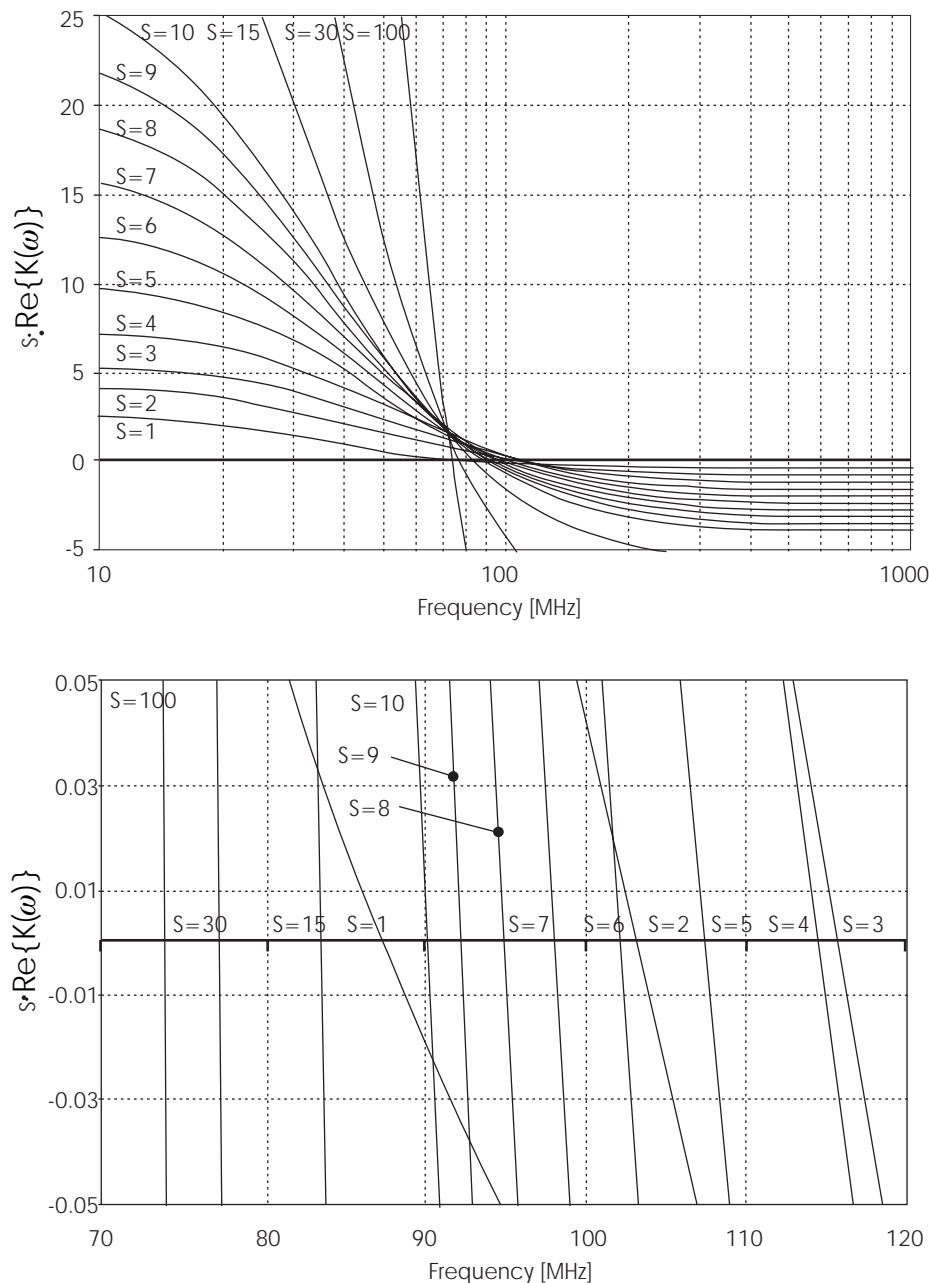


Figure 4. (a) Plot of the real part of the Classius-Mossoti factor times the erythrocyte stack number s , against the A.C. field frequency. The stack number s is a size parameter, meaning $s = 1$ a single erythrocyte, and $s > 2$ a linear cell aggregation of two or more erythrocytes. The conductivities and relative permittivities of the internal cell and the external medium are taken as 0.5 and 0.1 $S \times m^{-1}$, as well as 50 and 80, respectively^{17,30}. Particle dimensions are $2R = 7.5 \mu m$, $2L = s \times 2.2 \mu m$ with $s = 1, 2, 3, \dots$ characterizing the linear side-by-side adhesion of erythrocytes.

(b) Detail of the frequency region around the crossing through the line $s \cdot \text{Re}\{K(\omega)\} = 0$. The "crowding" of the curves belonging to $s = 1, 2, 3, 4$ is a consequence of the reorientation of very short rouleaux as described in the text.

We have not included in our study the effect of size- and shape dependent friction, which the particles might suffer in its movement. The friction factor of a sphere, a disk, a cube or a cylinder depends in a complicated way on geometrical and hydrodynamic conditions of the rheological system. While for a sphere-like particle the friction factor is known to be proportional to the sphere radius R , other cases are not so straight-forward. At any rate, the friction force counteracts and thus diminishes the DEP force on the considered particle.

In conclusion, existing microelectrode arrays for batch and continuous separation of microorganisms and cell should allow to achieve separation and sorting of a population of erythrocyte rouleaux. It is shown in this work, that the induced dipole moment in erythrocyte rouleaux of different level of aggregation causes a dielectrophoretic force effect, which is different in magnitude for different rouleaux lengths. Additionally exist frequency windows, where this force is negative for one subpopulation, while it is positive for another, providing

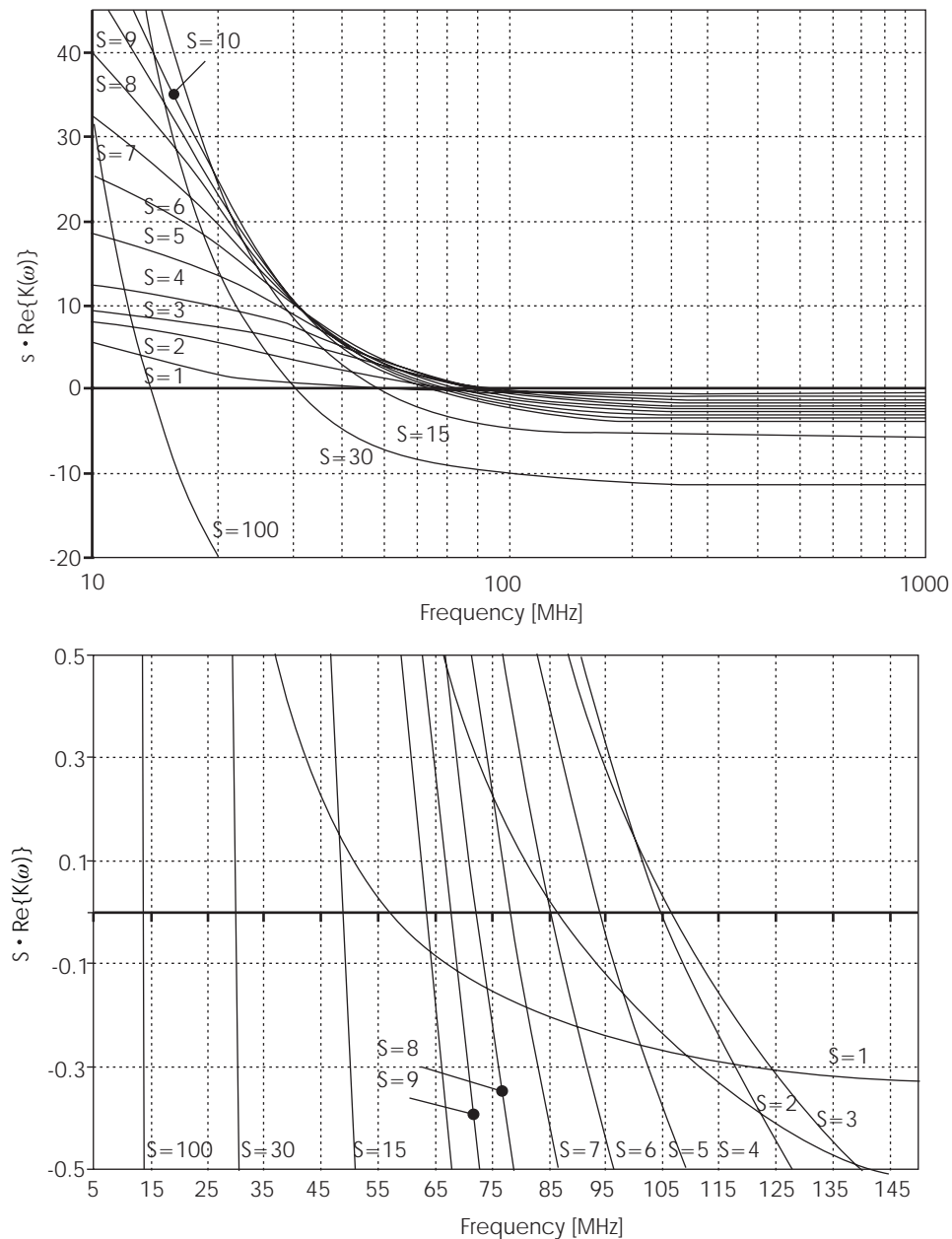


Figure 5. (a) Plot of the real part of the Classius-Mossoti factor times the erythrocyte stack number s , against the A.C. field frequency. Parameters are chosen as described in Figure 4, except the medium conductivity $\epsilon_m = 0.001$ S/m in this case. (b) Detail of the frequency region around the crossing through the line $s \times [\text{Re}\{K(\omega)\}] = 0$. The "crowding" of the curves belonging to $s = 1, 2, 3, 4$ is changed here as compared to Figure 4(b).

for a means of separation. In particular should dielectrophoretic field-flow-fractionation methods be suitable, where a differential positioning of particles within a suspension flow velocity profile is established by the action of corresponding dielectrophoretic forces.

BIBLIOGRAPHY

1. Foresto P, D'Arrigo M, Carreras L, Cuezco RE, Valverde J, Rasia R. Evaluation of red blood cell aggregations in diabetes by computerized image analysis. *Medicina*, 2000; 60: 570-572.
2. Baumier H, Neu B, Donath E, Kiesewetter H. Basic phenomena of blood cell rouleaux formation. *Biorheology* 1999; 36(5-6): 439-442.
3. Barshtein G, Wajnblum D, Yedgar S. Kinetics of linear rouleaux formation studied by visual monitoring of red cell dynamic organization. *Biophys J* 2000; 78(5): 2470-2474.
4. Bertoluzzo SM, Bollini A, Rasia M, Raynal A. Kinetic model for erythrocyte aggregation. *Blood Cells Mol Dis* 1999; 25(5-6): 339-349.
5. Riha P, Liao F, Stoltz JF. The effect of rouleaux formation on blood coagulation. *Clin Hemorrhol Microcorc* 1997; 17(4): 341-346.
6. Chien S, Sung LA, Kim S, Burke AM, Usami S. Determination of aggregation force in rouleaux by fluid mechanical technique. *Microvasc Res* 1977; 13(3): 327-333.

7. Pribush A, Meiselman HJ, Meyerstein D, Meyerstein N. Dielectric approach to investigation of erythrocyte aggregation. II. Kinetics of erythrocyte aggregation-disaggregation in quiescent and flowing blood. *Biorheology* 2000; 37(5-6): 429-441.
8. Ditenfass L. Experiment on "Discovery" STS 51-C: aggregation of red cells and thrombocytes in heart disease, hyperlipidaemia and other conditions. *Adv Space Res* 1989; 9(11): 65-69.
9. Baumler H, Neu B, Mitlohner R, Georgieva R, Meiselman HJ, Kiesewetter H. Electrophoretic and aggregation behavior of bovine, horse and human red blood cells in plasma and in polymer solutions. *Biorheology* 2001; 38(1): 39-51.
10. Baumann M. Dynamics of Oscillating Erythrocyte Doublets after Electrofusion. *Biophys J* 1999; 77(5): 2602-2611.
11. Priezhev AV, Forsov NN, Vyshlova MG, Lademann J, Richter H, Kiesewetter H, et al. Assessment of erythrocyte aggregation in whole blood samples by light backscattering: clinical applications. *SPIE Proceedings*, 1999; 3599.
12. Forsdyke DR, Ford PM. Segregation into separated rouleaux of erythrocytes from different species. Evidence against the agglomerin hypothesis of rouleaux formation. *Biochem J* 1983; 214: 257-260.
13. Chelidze T. Dielectric Spectroscopy of Blood: Experiment and Theory. Proc. 1st Int Conf on Diel. Spectroscopy in phys oil and oil Appl, (Jerusalem), 2001: 57.
14. Irimajiri A, Ando M, Matsuoka R, Ichinowatari T, Takeuchi S. Dielectric monitoring of rouleaux formation in human whole blood: a feasibility study. *Biochim Biophys Acta* 1996; 1290(3): 207-209.
15. Marx GH, Dyda PA, Pethig R. Dielectrophoretic separation of bacteria using a conductivity gradient. *J Biotechnol* 1996; 51: 175-180.
16. Morgan H, Hughes MP, Green NG. Separation of Submicron Bioparticles by Dielectrophoresis. *Biophys J* 1999; 77: 516.
17. Hughes MP, Morgan H, Rixon FJ, Burt JPH, Pethig R. Manipulation of herpes simplex virus type 1 by dielectrophoresis. *Biochim Biophys Acta* 1998; 1425: 119-126.
18. Talary M, Mills KI, Hoy T, Burnett AK, Pethig R. Dielectrophoretic separation and enrichment of CD34+ cell subpopulations from bone marrow and peripheral blood stem cells. *Med Biol Engl Comp* 1995; 33: 235-237.
19. Becker FF, Wang XB, Huang Y, Pethig R, Vykoukal J, Gascoyne PCR. The removal of human leukemia cell from blood using interdigitated microelectrodes. *J Phys D Appl Phys* 1994; 27: 2659-2662.
20. Marx GH, Pethig R. Dielectrophoretic separation of cells: continuous separation. *Biotechnol Bioeng* 1995; 45: 337-343.
21. Wang XB, Vykoukal J, Becker FF, Gascoyne PCR. Separation of polystyrene microbeads using dielectrophoretic/gravitational field-flow fractionation. *Biophys J* 1998; 74: 2689-2701.
22. Green NG, Morgan H. Dielectrophoretic investigations of submicrometre latex spheres. *J Phys D Appl Phys* 1997; 30: 2626-2633.
23. Washizu M, Kurosawa O, Arai I, Suzuki S, Shimamoto N. Applications of electrostatic stretch-and-positioning of DNA. *IEEE Trans Ind Appl* 1995; 31: 447-456.
24. Asbury CL, van den Engh G. Trapping of DNA in non-uniform oscillating electric fields. *Biophys J* 1998; 74: 1024-1030.
25. Voldman J, Braff RA, Toner M, Gray ML, Schmidt MA. Holding Forces of Single-Particle Dielectrophoresis Traps. *Biophys J* 2001; 80(1): 531-541.
26. Morgan H, Green NG, Huges MP, Tan TC. Large-area traveling wave dielectrophoresis particle separator. *J Micromech Microeng* 1997; 7: 65-70.
27. Jones TB. *Electromechanics of particles*. Cambridge University Press (Cambridge), 1995.
28. Ramos A, Morgan H, Green NG, Castellanos A. AC electrokinetics: a review of forces in microelectrode structures. *J Phys D Appl Phys* 1998; 31: 2338-2353.
29. Talary MS, Burt JPH, Tame JA, Pethig R. Electromanipulation and separation of cells using traveling electric fields. *J Phys D Appl Phys* 1996; 29: 2198-2203.
30. Pauly H, Suwan HP. Dielectric properties and ion mobility in erythrocyte. *Biophys J* 1966; 6: 621-39.
31. Bonincontro A, Gimsa J, Risuleo G, Rosa V. Critical analysis of the impedance method for the evaluation of permittivity and conductivity of the plasmamembrane. *Biologitscheski Membrany* 2000; 17: 102-106.
32. Kononenko VL, Ilyina TA. Dielectrodeformations of erythrocyte: Analysis of the ellipsoidal shear model. *Membr Cell Biol* 2001; 14(4): 537-551.
33. Morgan H, Green NG. Dielectrophoretic manipulation of rod-shaped viral particles. *J Electrostatics* 1997; 42: 279-293.
34. Gimsa J, Wachner D. A polarization model overcoming the geometric restrictions of the Laplace solution for spheroidal cell. *Biophys J* 1999; 77: 1316-1326.
35. Miller RD, Jones TB. Electro orientation of ellipsoidal erythrocytes. *Biophys J* 1993; 64: 1588-95.